HHS Public Access

Author manuscript

J Biomater Appl. Author manuscript; available in PMC 2015 December 06.

Published in final edited form as:

J Biomater Appl. 2015 November ; 30(5): 558–567. doi:10.1177/0885328215594704.

Effects of the orientation of anti-BMP2 monoclonal antibody immobilized on scaffold in antibody-mediated osseous regeneration

Sahar Ansari[1,2], **Marcelo Freire**[3], **Moon G Choi**[1], **Azadeh Tavari**[1], **Mohammad Almohaimeed**[4], **Alireza Moshaverinia**[2], and **Homayoun H Zadeh**[1]

[1]Laboratory for Immunoregulation and Tissue Engineering (LITE), Ostrow School of Dentistry of USC, University of Southern California, Los Angeles, CA, USA

[2]Center for Craniofacial Molecular Biology, Ostrow School of Dentistry of USC, University of Southern California, Los Angeles, CA, USA

[3]Department of Oral Medicine, Infection and Immunity, Harvard School of Dental Medicine, Boston, MA, USA

[4]Dental Research Center (DRC), Tissue Engineering and Biomaterials Research Unit (TEBRU), College of Dentistry, Qassim University, Qassim, Saudi Arabia

Abstract

Recently, we have shown that anti-BMP2 monoclonal antibodies (mAbs) can trap endogenous osteogenic BMP ligands, which can in turn mediate osteodifferentiation of progenitor cells. The effectiveness of this strategy requires the availability of the anti-BMP-2 monoclonal antibodies antigen-binding sites for anti-BMP-2 monoclonal antibodies to bind to the scaffold through a domain that will leave its antigen-binding region exposed and available for binding to an osteogenic ligand. We examined whether antibodies bound to a scaffold by passive adsorption versus through Protein G as a linker will exhibit differences in mediating bone formation. *In vitro* anti-BMP-2 monoclonal antibodies was immobilized on absorbable collagen sponge (ACS) with Protein G as a linker to bind the antibody through its Fc region and implanted into rat calvarial defects. The biomechanical strength of bone regenerated by absorbable collagen sponge/Protein G/anti-BMP-2 monoclonal antibodies immune complex was compared to ACS/anti-BMP-2 monoclonal antibodies or ACS/Protein G/isotype mAb control group. Results demonstrated higher binding of anti-BMP-2 monoclonal antibodies/BMPs to C2C12 cells, when the mAb was initially attached to recombinant Protein G or Protein G-coupled microbeads. After eight weeks, micro-CT and histomorphometric analyses revealed increased bone formation within defects implanted with absorbable collagen sponge/Protein G/anti-BMP-2 monoclonal antibodies compared with defects implanted with absorbable collagen sponge/anti-BMP-2 monoclonal antibodies ($p < 0.05$). Confocal laser scanning microscopy (CLSM) confirmed increased BMP-2, -4, and -7 detection in

Corresponding author: Homayoun H Zadeh, Laboratory for Immunoregulation & Tissue Engineering, Ostrow School of Dentistry, University of Southern California, 925 West 34th Street, Los Angeles, CA 90089, USA. zadeh@usc.edu.

Declaration of conflicting interests

None declared.

sites implanted with absorbable collagen sponge/Protein G/anti-BMP-2 monoclonal antibodies *in vivo*. Biomechanical analysis revealed the regenerated bone in sites with Protein G/anti-BMP-2 monoclonal antibodies had higher mechanical strength in comparison to anti-BMP-2 monoclonal antibodies. The negative control group, Protein G/isotype mAb, did not promote bone regeneration and exhibited significantly lower mechanical properties ($p < 0.05$). Altogether, our results demonstrated that application of Protein G as a linker to adsorb anti-BMP-2 monoclonal antibodies onto the scaffold was accompanied by increased *in vitro* binding of the anti-BMP-2 mAb/BMP immune complex to BMP-receptor positive cell, as well as increased volume and strength of *de novo* bone formation *in vivo*.

Keywords

Bone regeneration; biomaterials; chimeric anti-BMP2 monoclonal antibodies; tissue engineering; Protein G

Introduction

Repair and regeneration of bony defects is commonly accomplished using autologous, xenogenic and allogenic bone grafts.[1–3] Each of these graft materials has disadvantages that limit their application. Autogenous grafting has several drawbacks including: donor site morbidity, hematoma, pain, inflammation and the high cost of bone harvesting surgical procedures.[3–6] Xenogenic and allogenic grafts are osteoconductive and have limited ability to regenerate bone, in particular in larger defects. Biologics, such as recombinant human bone morphogenetic proteins (rhBMPs), including rhBMP-2 and rhBMP-7 have been applied clinically, because of their osteoinductive potential.[7–9] Nonetheless, these growth factors also have their own limitations, including lower biological activity than their endogenous counterparts, inability to sustain effective local concentrations, necessitating application of supraphysiologic doses, as well as high cost.[9–13] Therefore, alternative bone regenerative treatment modalities are required. The ultimate goal of bone tissue engineering is to develop biological bone constructs, with similar physical and biological properties of natural bone tissue, which restore, maintain, or improve bone tissue function.[3–7,14]

Recently, our research group has introduced a novel tissue engineering method involving application of anti-BMP-2 monoclonal antibody (mAb) immobilized on scaffolds in an effort to capture endogenous BMP-2.[15–18] Our data have demonstrated the *in vivo* capturing of endogenous BMP-2, -4 and -7 by anti-BMP-2 mAb, as well as *de novo* bone formation.[15–17] This approach was termed antibody-mediated osseous regeneration (AMOR). Our previous studies have demonstrated ability of both murine-derived,[15–17] as well as chimeric anti-BMP2 monoclonal antibodies to be effective in AMOR.[18]

Stork et al. in their studies reported that fusing a single-chain diabody to an albumin-binding domain from streptococcal Protein G improved the circulation time by a factor of 6.[19] Therefore, we have hypothesized that anti-BMP-2 mAb captures BMPs, which are then presented to their cellular receptors, triggering their osteogenic differentiation. This will require availability of the antigen-binding region of antibody to bind to BMPs in domain(s), which do not interfere with interactions with their cellular receptors. To begin to further test

this hypothesis, it was sought to determine whether binding of anti-BMP-2 mAb to the scaffold through its Fc region may be a more effective strategy, since this is likely to leave antigen-binding sites available to binding BMP ligands. To that end, Protein G, which is a bacterial cell wall protein with specific affinity for immunoglobulin (IgG) was utilized. If confirmed, this information will have utility in optimizing AMOR for translational applications.

Materials and methods

Antibodies and Protein G

We generated and used a chimeric anti-BMP2 IgG2 mAb according to the method previously reported.[18] An isotype-matched mAb (Iso mAb) with no specificity for BMP2 was utilized as the negative control. The rec-Protein G (Recombinant Protein G from *E. coli*, Invitrogen, Carlsbad, CA) and μMACS Protein G-coupled microbeads (Miltenyi Biotec Inc., Auburn, CA) were utilized in this study.

Cell culture and flow cytometry

C2C12 mouse myoblast cell line (American Type Culture Collection) was used in this study. C2C12 cells were cultured in Dulbecco's modified Eagle's medium (Sigma-Aldrich) supplemented with 100 units/mL penicillin, 100 mg/mL streptomycin (Sigma-Aldrich) and 10% fetal bovine serum (Biocell Laboratories, Rancho Dominguez, CA) at 37°C in a humidified atmosphere supplied with 5% CO_2.

A flow cytometric assay was developed in order to study binding of the BMP2 cellular receptor with the immune complex formed between chimeric anti-BMP2 mAb/BMP-2 and rec-Protein G or Protein G-coupled microbeads. Briefly, chimeric anti-BMP2 mAb (25 μg/mL) or isotype-matched control mAb (25 μg/mL) was incubated with Protein G-coupled microbeads, washed with PBS, and non-specific binding sites were blocked with bovine serum albumin (0.5 mg/mL BSA, Invitrogen). Then rhBMP-2 (100 ng/mL, Medtronic, Minneapolis, MN) was incubated with mAb/Protein G complex for 30 min at 4°C, and was washed thoroughly with PBS to remove free rh-BMP-2 ligand. The resultant immune complexes were then incubated with C2C12 cells (American Type Culture Collection, Manassas, VA), which express BMP-2 receptors. Subsequently, the immune complexes were immunolabeled using phycoerythrin-conjugated goat anti-human Ab (Santa Cruz Biotchnology, Dallas, TX). The intensity of fluorescent labeling was determined by measuring mean fluorescent intensity (MFI) using a flow cytometer (FACS Calibur; Becton Dickinson, Laguna Hills, CA). Controls included cells alone (−) and substitution of anti-BMP2 mAb with isotype-matched mAb with no specificity (isotype mAb).

In vitro release kinetics study

In order to evaluate the kinetics of chimeric anti-BMP2-Protein G complex release from ACS scaffold, 25 μg/mL of either chimeric mAb or chimeric anti-BMP2-Protein G complex was adsorbed on ACS scaffold. Subsequently, the mAb or chimeric mAb-Protein G complex-loaded scaffolds were suspended in 5 mL of PBS (pH = 7.4). At various time points (1, 3, 7 and 14 days), the amount of released mAb was determined by UV absorption

spectroscopy (Beckman, Brea CA). Furthermore, the retained mAb was detected with FITC-conjugated goat anti-human IgG antibody (Santa Cruz Biotechnology Inc, CA) using immunofluorescence microscopy.

In vivo study

The USC Institutional Animal Care and Use Committee approved all procedures involving vertebrate animals. Two-month-old virgin female Sprague-Dawley rats (n = 24, Harlan Laboratories, Livermore, CA) were housed at 22°C under a 12 h light and 12 h dark cycle and fed ad libitum (Purina Inc, Baldwin Park, CA). Calvarial defects were created in eight-week-old rats under general anesthesia administered by IP injection of ketamine/xylazine 80–90 mg/kg, 5–10 mg/kg. Full-thickness skin flaps were raised, exposing the left and right parietal bones. Defects in the midline of the parietal bone, 7 mm in diameter, were generated using a trephine under copious saline irrigation. Protein G-coupled microbeads were incubated with ACS scaffold for an hour, washed three times with PBS and incubated with anti-BMP2 mAb (25 μg/mL) to form anti-BMP2-Protein G complex on ACS. Subsequently, ACS scaffolds were surgically implanted into rat calvarial defects. For comparison, anti-BMP2 mAb adsorbed directly on ACS scaffolds (25 μg/mL), as the positive control group, and isotype control mAb with no specificity (25 μg/mL) as the negative control, were used in the calvaria defect model. After eight weeks, the animals were sacrificed in a CO_2 chamber and the skulls were harvested and stored in buffered formalin while awaiting analysis. In order to confirm our hypothesis, another type of Protein G, rec-Protein G (Recombinant Protein G from *E. coli*, Invitrogen) was utilized in another series of rat calvarial defect model.

Micro-CT analysis

Upon sacrifice at eight weeks following transplantation, the calvarial defects were examined using a high-resolution micro CT system (MicroCAT II, Siemens Medical Solutions Molecular Imaging, Knoxville, TN) to evaluate the healing of the defects. The specimens were scanned every 10 μm at 60 kV and 110 μA at a spatial resolution of 18.7 μm (Voxel dimension) and three-dimensional (3D) histomorphometric analysis was performed on the resulting images. Bone volume fraction divided by total volume (BV/TV) of newly regenerated bone for each specimen was calculated using Amira software (Visage Imaging Inc., San Diego, CA).

Histological and histomorphometric analysis

For histological analysis, the retrieved specimens were fixed with 4% (v/v) paraformaldehyde for 30 min at room temperature and placed in PBS for 15 min prior to dehydration. Serial dehydration was achieved by placing specimens in a sequential series of increasing ethanol concentrations to remove all of the water. The ethanol was then completely replaced with a series of solutions containing increasing concentrations of xylene, culminating in 100% xylene, prior to incubation with paraffin-saturated xylene at room temperature overnight. The specimens were then serially sectioned (6 μm) and affixed to glass slides. Additionally, the paraffin was completely removed by immersion in xylene, followed by immersion in decreasing ethanol concentrations and then washing with tap

water. The sections were stained with Hematoxylin and Eosin (H&E). Images were captured using an Olympus DP50 digital camera (Olympus Optical Co, Japan) and analyzed using Analysis imaging software (Soft Image System GmbH, Germany).

Immunofluorescence staining

The rats were scarified eight weeks after transplantation and harvested specimens were prepared according to previous publications.[16,17] Briefly, specimens were treated with 3% H_2O_2, followed by a blocking buffer (1% BSA and 0.25% Triton X-100 in PBS). Specimens were then incubated with rat anti-rabbit anti-BMP2, -BMP4, and -BMP7 (Abcam, 1:200 dilution) and detected using Alexa Fluor conjugated secondary antibody (Invitrogen, 1:200 dilution). The samples were then counterstained with DAPI. The positively stained areas were determined from three independent samples for each experimental group. Five areas were randomly selected from each sample, and then the positive area in the field was calculated with NIH Image-J software (NIH, Bethesda, MD) and shown as a percentage of the area over total field area.

Biomechanical analysis

Eight weeks post implantation surgery, the rats were sacrificed and the implanted scaffolds with a layer of surrounding bone were removed using a trephine drill and the host bone surrounding the implants was trimmed with dental burs, leaving a disc-shaped specimen. These boney specimens were then rinsed in physiological saline and stored in sterile plastic containers with saline at 4°C. The mechanical response of the implants was evaluated using a universal mechanical testing machine (Instron, Norwood, MA). The specimens were secured in position while the load was applied vertically, by a steel rod with a diameter of 2 mm, to the center of the former defect (compression rate = 0.5 mm min^{-1}) (n = 4). During compression, load–deformation values were recorded and stored with the computer software supplied with the testing machine. The fracture strength (Fmax) was determined as the maximum force applied to cause fracture of the healed defect site.[20,21]

Statistical analysis of data

Quantitative data were expressed as mean±standard deviation (SD). One-way and two-way analyses of variance (ANOVA) followed by Tukey's test at a significance level of $\alpha = 0.05$ were used for the comparison among multiple sample means.

Results

In vitro binding of Protein G/anti-BMP2 mAb complex with BMPs

In order to determine whether the orientation of available antibody can affect binding and accumulation of endogenous BMP-2 and other cross-reactive BMPs, rec-Protein was incubated with anti-BMP2 mAb (Figure 1). The anti-BMP2 mAb bound to Protein G was incubated with BMP-2. The binding of Protein G/mAb/BMP immune complexes to C2C12 cells with BMP cellular receptor was studied by flow cytometry. Results of flow cytometric analysis revealed significantly higher binding of immune complexes between anti-BMP-2 mAb and C2C12 cells, when the mAb was previously bound to recombinant Protein G (Figure 2). Since mAb binds to Protein G through its Fc region, the increased binding of the

Protein G/anti-BMP-2 mAb/rhBMP-2 immune complex to C2C12 cells may be attributed to preferential availability of antigen-binding sites on anti-BMP-2 mAb. Alternatively, binding of mAbs to microbeads may be responsible for increased binding to C2C12 cells because it clusters mAb molecules together on microbeads. Same trend was observed for the flow cytometric analysis using rec-Protein G (not shown).

In vitro binding and release characteristics of anti-mAb Protein G complex

To examine potential differences in the binding and release profile of the chimeric mAb or chimeric mAb Protein G complex on ACS scaffold, an *in vitro* binding and release kinetics study was performed. Results demonstrated sustained release of anti-BMP-2 mAb or Protein G/anti-BMP-2 mAb immune complex for up to 14 days (Figure 3(a)). Additionally, no statistically significant difference was found in the levels of the mAb detected on ACS scaffold after 14 days (Figure 3(b)). These results confirmed that when Protein G (either recombinant or Protein G coupled to microbeads) is used as linker for binding of anti-BMP-2 mAb to ACS, release of the mAb from the ACS scaffold is not inhibited.

In vivo osteogenic properties of Protein G/anti-BMP2 mAb complex

To determine the effects of orientation of binding of anti-BMP-2 to scaffold, Protein G-coupled microbeads were first incubated with ACS, followed by incubation with anti-BMP-2 mAbs. The ACS/Protein G/anti-BMP-2 mAb or ACS/Protein G/isotypic mAb, ACS/anti-BMP-2 mAb or ACS/isotypic mAb were each implanted into critical size rat calvarial defects. After eight weeks, healing of calvarial defects was studied by micro-CT and histology. Micro-CT analysis (Figure 4(a)) showed increased volume of bone formation within calvarial defects implanted with ACS/Protein G/anti-BMP2 mAb in comparison to the defects implanted with anti-BMP2 mAb adsorbed directly on ACS ($p < 0.05$) (Figure 4(b)). Substitution of anti-BMP-2 mAb with isotype control mAb with or without Protein G was not associated with any significant bone formation.

Histological results demonstrated the presence of vital bone with osteocytes in lacunae within defect sites implanted with Protein G/anti-BMP2 mAb complex adsorbed onto ACS scaffolds, as well as ACS with anti-BMP-2 mAb (Figure 5(a)). No evidence of bone formation was observed in sites implanted with isotype-matched control mAb with or without Protein G. Histomorphometric analysis (Figure 5(b)) revealed increased volume of bone formation within calvarial defects implanted with Protein G/anti–BMP2 mAb in comparison to the defects implanted with anti–BMP2 mAb adsorbed directly to ACS ($p < 0.05$) or isotype control mAb ($p < 0.05$).

To confirm that the presence of Protein G-coupled microbeads led to increased osteogenic activity of Protein G/anti-BMP2 mAb, another form of Protein G(rec-Protein G) was utilized instead in the same experiments described above. Micro-CT (Supplementary Figure s1(a) and (b)) and histological analyses (Supplementary Figure s2(a) and (b)) showed increased amounts of bone formation within calvarial defects implanted with rec-Protein G/anti-BMP2 mAb/ACS in comparison to the defects implanted with anti-BMP2 mAb adsorbed directly on ACS ($p < 0.05$) or rec-Protein G/isotype control mAb ($p < 0.05$).

To further characterize the phenotype of regenerated tissues in response to the application of Protein G as a linker for adsorbing anti-BMP-2 mAb on ASC scaffold, immunofluorescence labeling was utilized. Representative sites implanted with ACS/Protein G/anti-BMP2 mAb complex or ACS/anti–BMP2 mAb, exhibited high BMP2, BMP4 and BMP7 protein expression throughout regenerated tissues (Figure 6(a)). As expected, within sites implanted with isotype control mAb no appreciable BMP-2, BMP-4, or BMP-7 was detected (Figure 6(a)). Semi-quantitative analysis revealed higher detection of BMP-2, -4 and -7 proteins within sites implanted with Protein G/anti-BMP2 mAb complex than those with anti-BMP2 mAb adsorbed directly on ASC ($p < 0.05$) or non-specific isotype control mAb ($p < 0.05$) (Figure 6(b)).

One of the important considerations is potential adverse effects of antibodies or Protein G. In order to examine the safety of *in vivo* administration of anti-BMP-2 mAb with and without Protein G linker, histologic specimens were carefully examined for any signs of adverse reactions. To rule out such potential adverse effects, serial histological slides were carefully examined for increased inflammatory infiltrate or any other aberrant tissue morphology. No such adverse reactions were noted in any of the histologic sections from any of the intervention groups.

Biomechanical evaluation of regenerated bone

One of the key properties of regenerated bone is its biomechanical strength, in particular in load-bearing regions. To that end, the present study sought to compare the biomechanical properties of bone regenerated by antibody-mediated bone regeneration process when Protein G was used as a linker for binding to scaffold, to when Protein G was not used. Accordingly, the critical size calvarial defect model was used, where defects were implanted with one of five scaffolds, namely (1) ACS/Protein G/anti-BMP-2 mAb, (2) ACS/anti-BMP-2 mAb, (3) ACS/Protein G/isotype control mAb, (4) ACS/isotype control mAb or (5) ACS/rhBMP-2 as positive control. Calvarial specimens were harvested after eight weeks of healing and the degree of force required to induce mechanical failure (Fmax) was measured and compared for all the groups. Results demonstrated that groups implanted with ACS/Protein G/anti-BMP-2 mAb immune complex, exhibited higher values for Fmax in comparison to the groups implanted with anti-BMP-2 mAb or ACS/anti-BMP-2 mAb ($p < 0.05$) and ACS/Protein G/isotype control mAb ($p < 0.05$) (Figure 7). The data also showed that the strength of bone regenerated with anti-BMP-2 mAb was dependent on the orientation of the antibody dictated by Protein G linker. In order to gain better perspective about the strength of the regenerated bone, the ratio of the Fmax of regenerated bone to that of native bone was calculated. These data revealed that ACS/Protein G/anti-BMP-2 mAb, ACS/anti-BMP-2 mAb and ACS/Protein G/isotype control mAb were able to achieve 48%, 43% and 6% of the biomechanical strength of native bone, respectively (Figure 7). rhBMP-2 with ACS, used as positive control achieved 50% of the strength of native bone.

Discussion

FDA has approved recombinant human BMP-2 and -7 for specific indications in bone reconstruction. However, the clinical applications of these exogenous recombinant growth

factors are fraught with potential negative outcomes. Therefore, Freire et al. introduced the concept of AMOR as a tissue engineering alternative to administration of exogenous growth factors.[16,17] More recently, Ansari et al. generated a chimeric anti-BMP-2 mAb to reduce the potential for xenogenic immune response to the mAb. In their study, it was confirmed the ability of chimeric anti-BMP-2 mAb immobilized on different types of biomaterials to mediate robust *de novo* bone formation in rat calvarial defects.[18] In an attempt to optimize AMOR, it was sought to determine whether the orientation with which antibody is adsorbed onto the scaffold could affect the safety and efficacy of AMOR. It may be envisioned that optimization of AMOR will require maximal availability of antigen-binding sites on anti-BMP-2 mAb molecules. Moreover, it may be speculated that exposure of Ab Fc regions can potentially allow binding of inflammatory cells. To that end, Protein G was used as a linker for anti-BMP-2 mAb molecules onto scaffold. This will allow binding of the anti-BMP-2 mAb through its Fc receptor to expose the antigen-binding sites and limit the exposure of Fc regions. Our release profile characterization demonstrated sustained release of anti-BMP-2 mAb Protein G complex adsorbed on ACS scaffold.

Careful analysis of histological sections failed to demonstrate any significant inflammatory immune response within sites implanted with anti-BMP-2 mAb/Protein G/ACS or anti-BMP-2 mAb/ACS. These results are consistent with our previous observations regarding lack of significant inflammatory immune response associated with AMOR. Moreover, immunofluorescence staining data confirmed that the application of G protein as a linker for anti-BMP-2 to ACS scaffold leads to increased expression and/or accumulation of BMP-2, BMP-4, and BMP-7 ligands within reconstructed tissues, while specimens immobilized with anti-BMP2 mAb alone showed significantly less amounts of positive staining.

The present study utilized Protein G to control the orientation of binding of anti-BMP-2 mAb to scaffold. It is well known that this bacterial cell wall protein is a more versatile IgG-binding molecule compared with staphylococcal Fc-binding protein A.[22,23] Compared with protein A, the magnitude of the binding properties and the range of specificities of Protein G may prove to be of great value, not only when the use of protein A is limited but also as an improvement in applications already developed for protein A.[22–25] In addition, in our mechanical analysis, the maximum load to fracture was determined as the maximum force applied during the biomechanical test, which is the force applied to cause fracture of the healed defect site. The results demonstrated that the strength of bone regenerated with anti-BMP-2 mAb was dependent on the orientation of the antibody dictated by Protein G linker. The presence of Protein G and anti-BMP-2 mAb significantly increased the strength of the regenerated bone in comparison to other tested groups. It has to be mentioned that by application of ACS/Protein G/anti-BMP-2 mAb immune complex, we were able to regenerate up to 63% of the strength of native bone, which is very significant in clinical application in stress bearing areas.

Altogether, our present data have confirmed that the application of Protein G as a linker increased both *in vitro* binding of anti-BMP-2 mAb/BMP immune complexes to cells, as well as *in vivo* repair of calvarial critical size defects. The present study provided experimental evidence for the significance of the orientation of anti-BMP-2 in antibody-

mediated bone regeneration. Follow-up studies are under way to determine the molecular mechanisms by which anti-BMP-2 modulates the healing response of bone defects.

Conclusion

In this study, it was shown that when Protein G was used as a linker to mediate adsorption of anti-BMP2 mAb through its Fc region to scaffold, the *in vivo* capacity of anti-BMP2 mAb to bind to BMP-2, -4 and -7 was significantly increased. Moreover, the application of Protein G in binding anti-BMP2 mAb was associated with increased bone regeneration with higher biomechanical strength in critical size calvarial defects. Moreover, the ability of ACS/Protein G/anti-BMP-2 mAb immune complex to achieve 63% of the biomechanical strength of native bone demonstrated that this modality of treatment is an effective tissue engineering approach.

Acknowledgments

Funding

The first author (SA) was supported by a NIDCR postdoctoral training grant (T90DE021982), while AM was supported by a grant from the National Institute of Dental and Craniofacial Research (K08DE023825).

References

1. Chen FM, Zhang J, Zhang M, et al. A review on endogenous regenerative technology in periodontal regenerative medicine. Biomaterials. 2010; 31:7892–7927. [PubMed: 20684986]
2. Monaco E, Bionaz M, Hollister SJ, et al. Strategies for regeneration of the bone using porcine adult adipose-derived mesenchymal stem cells. Theriogenology. 2011; 75:1381–1399. [PubMed: 21354606]
3. Moshaverinia A, Chen C, Xu X, et al. Regulation of the stem cell–host immune system interplay using hydrogel coencapsulation system with an anti inflammatory drug. Adv Funct Mater. 2015; 25:2296–2307. [PubMed: 26120294]
4. Moshaverinia A, Chen C, Xu X, et al. Bone regeneration potential of stem cells derived from periodontal ligament or gingival tissue sources encapsulated in RGD-modified alginate scaffold. Tissue Eng Part A. 2014; 20:611–621. [PubMed: 24070211]
5. Arrington ED, Smith WJ, Chambers HG, et al. Complications of iliac crest bone graft harvesting. Clin Orthop Relat Res. 1996; 329:300–309. [PubMed: 8769465]
6. Sachlos E, Czernuszka JT. Making tissue engineering scaffolds work. Review on the application of solid free-form fabrication technology to the production of tissue engineering scaffold. Eur Cell Mater. 2003; 5:29–40. [PubMed: 14562270]
7. Betz VM, Betz OB, Harris MB, et al. Bone tissue engineering and repair by gene therapy. Front Biosci. 2008; 13:833–841. [PubMed: 17981592]
8. Kretlow JD, Young S, Klouda L, et al. Injectable biomaterials for regenerating complex craniofacial tissues. Adv Mater. 2009; 21:3368–3379. [PubMed: 19750143]
9. Zhu W, Rawlins BA, Boachie-Adjei O, et al. Combined bone morphogenetic protein-2 and -7 gene transfer enhances osteoblastic differentiation and spine fusion in a rodent model. J Bone Miner Res. 2004; 19:2021–2032. [PubMed: 15537446]
10. Chin M, Ng T, Tom W, et al. Repair of alveolar clefts with recombinant human bone morphogenetic protein (rhBMP-2) in patients with clefts. J Craniofac Surg. 2005; 16:778–790. [PubMed: 16192856]
11. Wikesjo UM, Polimeni G, Qahash M. Tissue engineering with recombinant human bone morphogenetic protein-2 for alveolar augmentation and oral implant osseointegration:

experimental observations and clinical perspectives. Clin Implant Dent Relat Res. 2005; 7:112–129. [PubMed: 15996358]

12. Khan S, Lane J. The use of recombinant human bone morphogenetic protein-2 (rhBMP-2) in orthopaedic applications. Expert Opin Biol Ther. 2004; 4:741–753. [PubMed: 15155165]
13. Chen D, Zhao M, Mundy G. Bone morphogenetic proteins. Growth Factors. 2004; 22:233. [PubMed: 15621726]
14. Porter JR, Ruckh TT, Popat KC. Bone tissue engineering: a review in bone biomimetics and drug delivery strategies. Biotechnol Prog. 2009; 25:1539–1560. [PubMed: 19824042]
15. Oldham J, Lu L, Zhu X, et al. Biological activity of rhBMP-2 released from PLGA microspheres. J Biomech Eng. 2000; 122:289–292. [PubMed: 10923299]
16. Freire MO, You HK, Kook JK, et al. Antibody-mediated osseous regeneration: a novel strategy for bioengineering bone by immobilized anti-bone morphogenetic protein-2 antibodies. Tissue Eng Part A. 2011; 17:2911–2921. [PubMed: 21870943]
17. Freire MO, Kim HK, Kook JK, et al. Antibody-mediated osseous regeneration: the early events in the healing response. Tissue Eng Part A. 2013; 17:254–262.
18. Ansari S, Moshaverinia A, Pi SH, et al. Functionalization of scaffolds with chimeric anti-BMP-2 monoclonal anti-bodies for osseous regeneration. Biomaterials. 2013; 34:10191–10198. [PubMed: 24055525]
19. Stork R, Muller D, Kontermann RE. A novel tri-functional antibody fusion protein with improved pharmacokinetic properties generated by fusing a bispecific single-chain diabody with an albumin-binding domain from streptococcal protein G. Protein Eng Des Sel. 2007; 20:569–576. [PubMed: 17982179]
20. Spicer PP, Kretlow JD, Young S, et al. Evaluation of bone regeneration using the rat critical size calvarial defect. Nat Protoc. 2012; 7:1918–1929. [PubMed: 23018195]
21. Jones L, Thomsen JS, Mosekilde L, et al. Biomechanical evaluation of rat skull defects, 1, 3, and 6 months after implantation with osteopromotive substances. J Craniomaxillofac Surg. 2007; 35:350–357. [PubMed: 17951064]
22. Erntell M, Myhre EB, Sjobring U, et al. Streptococcal protein G has affinity for both Fab and Fc-fragments of human IgG. Mol Immunol. 1988; 2:121–126. [PubMed: 3131664]
23. Reis KJ, Hansen HF, Bjorck L. Extraction and characterization of IgG Fc receptors from group C and group G streptococci. Mol Immunol. 1986; 23:425–431. [PubMed: 3724759]
24. Akerstorm B, Brodin T, Reis K, et al. Protein G: a powerful tool for binding and detection if monoclonal and polyclonal antibodies. J Immunol. 1985; 135:2589–2592. [PubMed: 4031496]
25. Grubb A, Grubb R, Christensen P, et al. Isolation and some properties of an IgC Fc-binding protein from group A streptococci type 15. Int Arch Allergy Appl Immunol. 1985; 67:369–386. [PubMed: 6461610]
26. Moshaverinia A, Ansari S, Chen C, et al. Co-encapsulation of anti-BMP2 monoclonal antibody and mesenchymal stem cells in alginate microspheres for bone tissue engineering. Biomaterials. 2013; 34:6572–6579. [PubMed: 23773817]

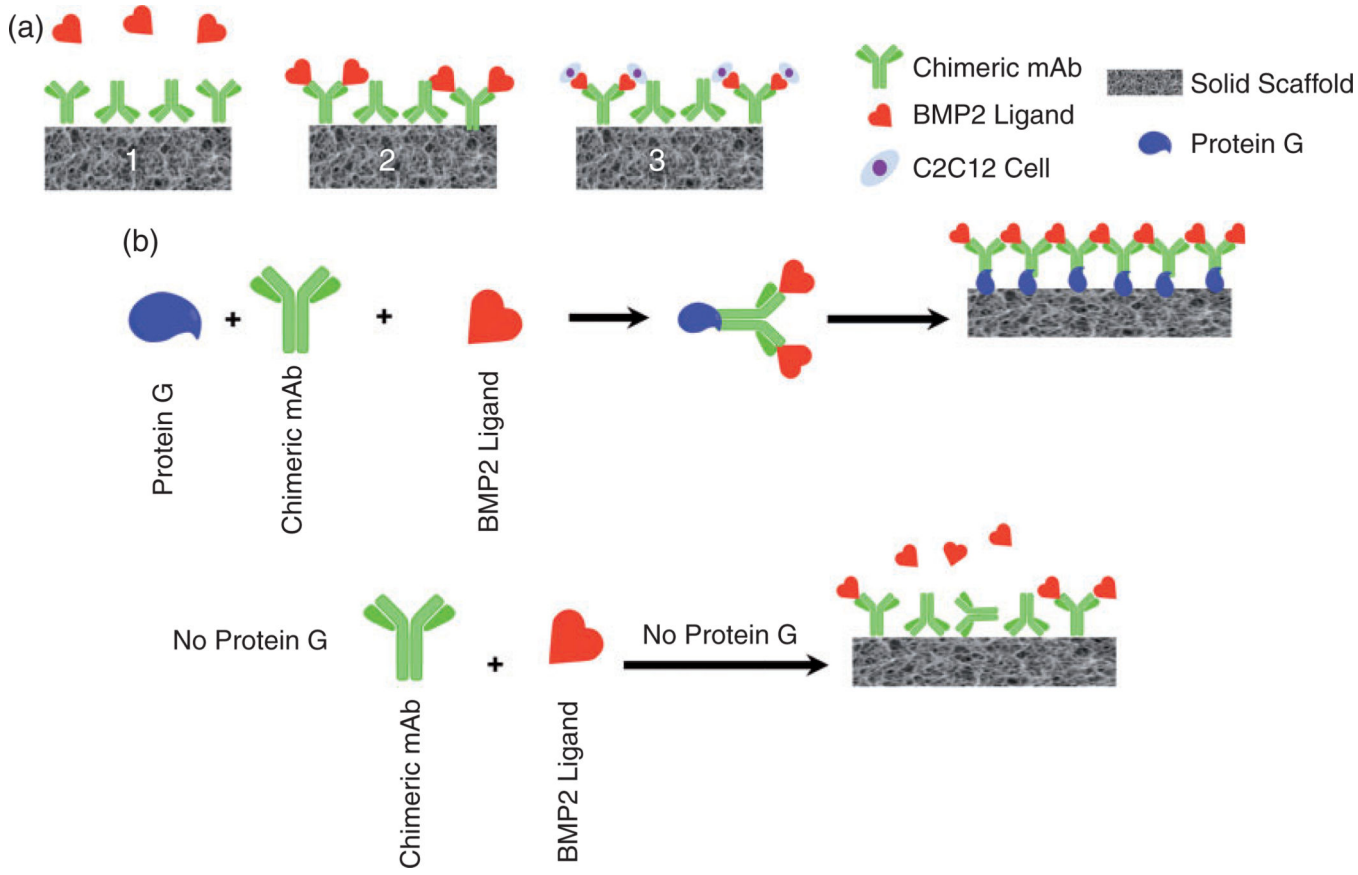

Figure 1.

(a) AMOR: (1) anti-BMP-2 mAb is immobilized on a scaffold. (2) mAb captures endogenous BMP-2 (and other homologous osteogenic BMPs) from the microenvironment. (3) BMP-2 captured by specific mAb binds its cellular receptor on osteoprogenitor cells, promoting their osteogenic differentiation. (b) Schematic representation of the binding of the immune complex (IC) between Protein G/anti-BMP-2 mAb/BMP's to cellular receptors *in vivo*.

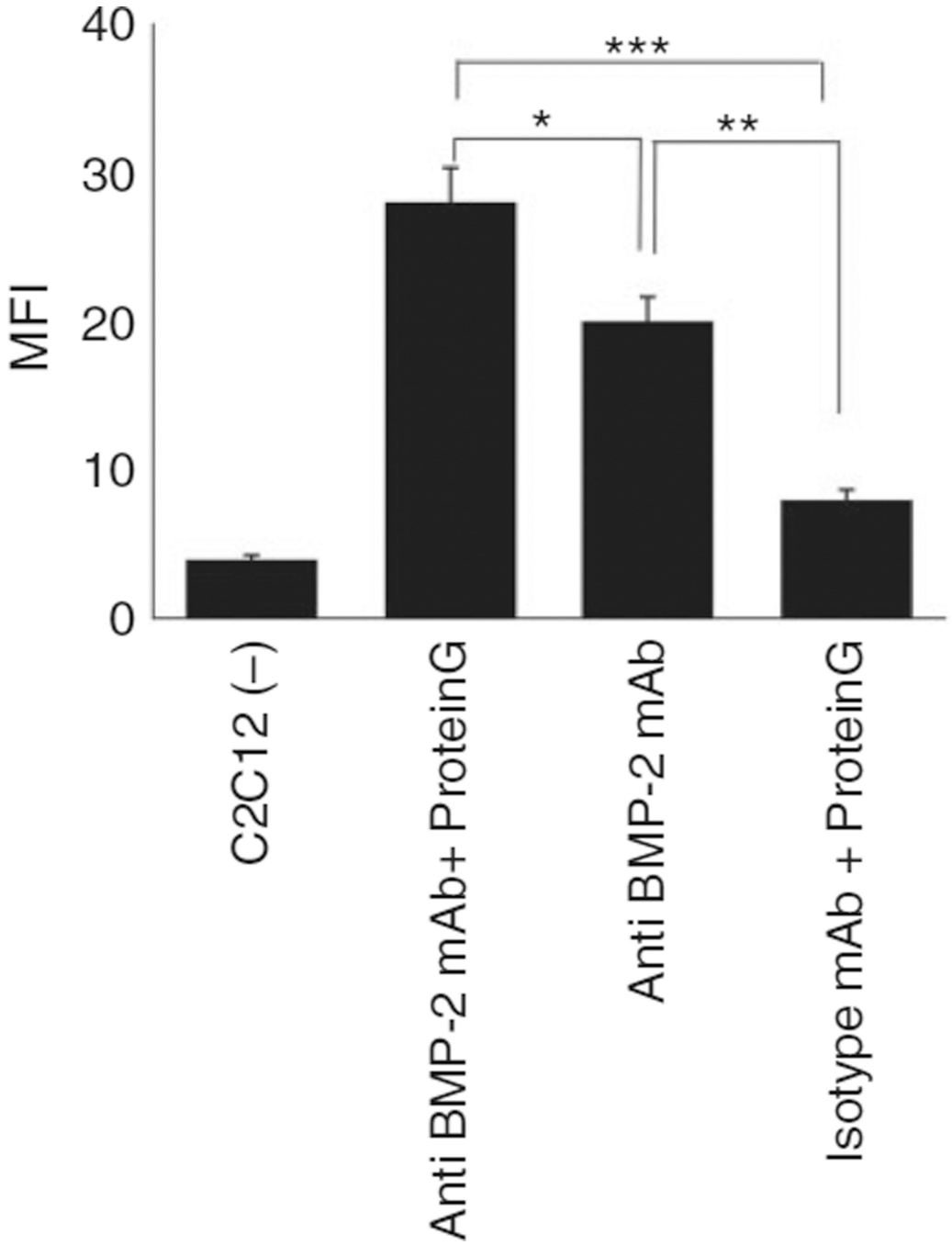

Figure 2.

Investigation of the effect of orientation of anti-mAb on the binding of the immune complex of anti-BMP2/BMP2 to target cells. Flow cytometric analysis of binding of the immune complex between anti-BMP-2 mAb/recombinant protein-G/BMP-2, BMP-4 or BMP-7/BMP-2 cellular receptor on C2C12 cells. Fluorochrome-labeled cells were analyzed by flow cytometer and the mean fluorescence intensity (MFI) of PE was calculated. Controls included cells alone (−) or substitution of chimeric anti-BMP2 mAb with isotype-matched

Ab (Iso mAb). The MFI of flowcytometric analysis showed significant binding between PG/chimeric antibody complex and BMP2.
**$p < 0.01$, and ***$p < 0.001$.

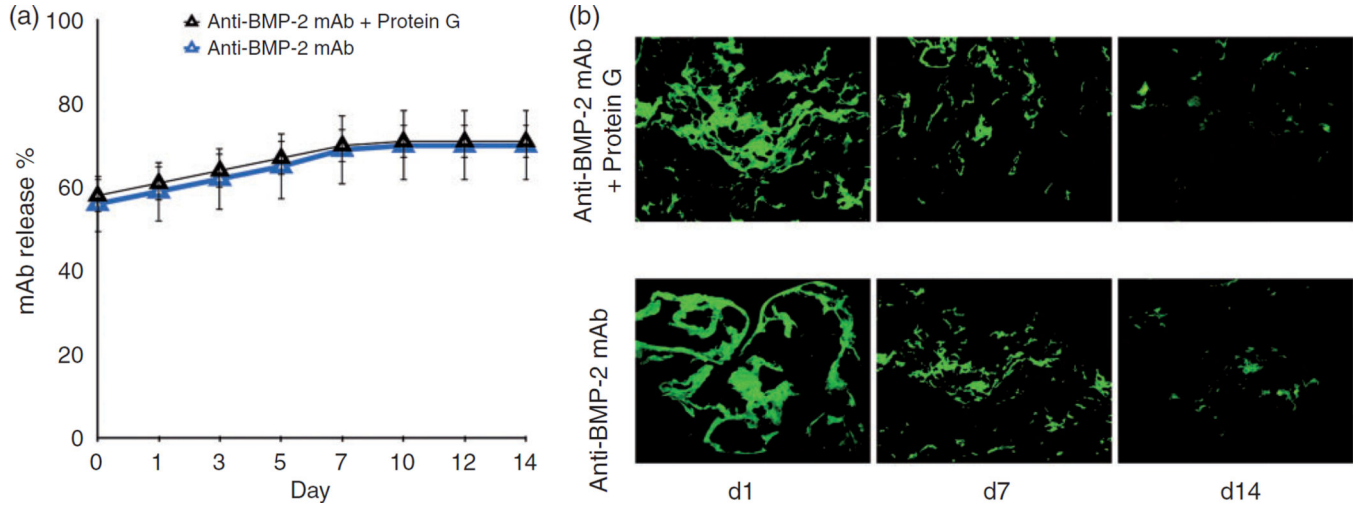

Figure 3.

Characterization of the *in vitro* release profile and binding of chimeric mAb and chimeric mAb Protein G complex-loaded scaffolds. (a) The *in vitro* release of mAb was calculated by measuring mAb concentrations in solution at various time points. (b) Fluorescence microscopic analysis demonstrating binding of anti-BMP-2 mAb on ACS scaffold detected by FITC-conjugated goat anti-human secondary antibody at different time intervals.
$^{*}p < 0.05$.

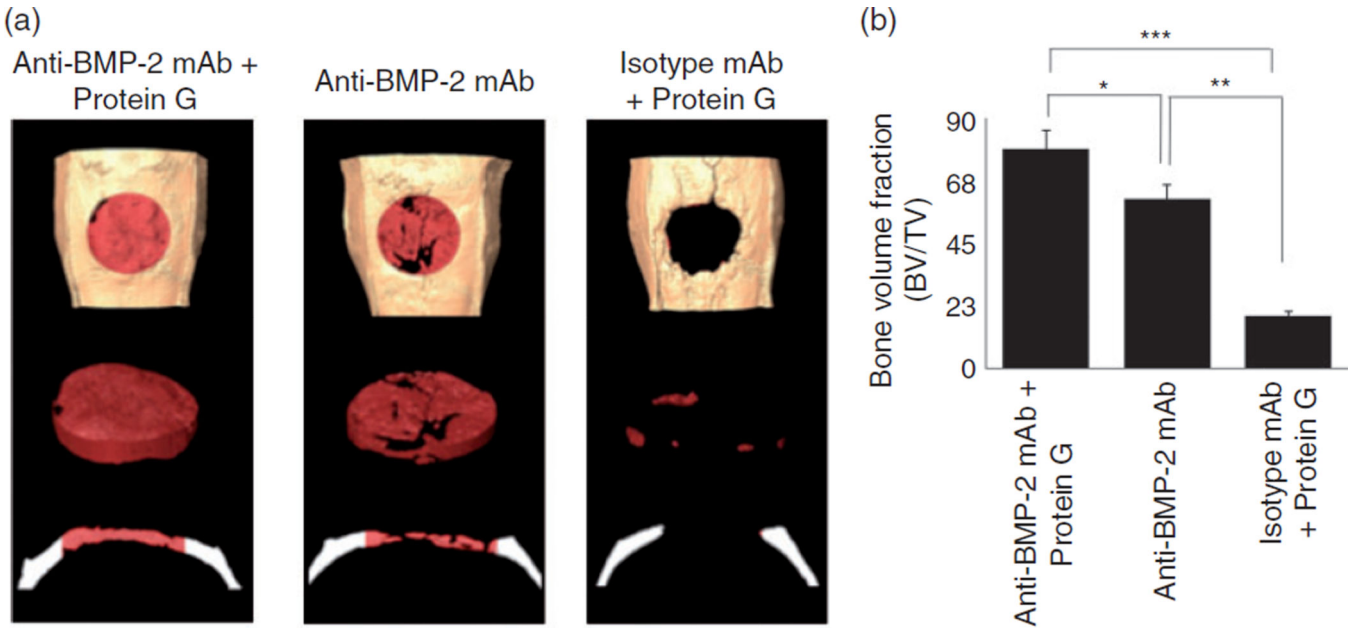

Figure 4.

(a) Representative 3D reconstruction of micro-CT images of bone volume within rat calvaria. Anti-BMP-2 mAb immobilized on ACS with or without Protein G-coupled microbeads linker implanted within rat calvarial defects. Isotype-matched mAb immobilized on ACS served as the control. (b) Bone volume/total volume (BV/TV) within calvarial defects in each specimen was measured by micro-CT.

*$p < 0.05$, **$p < 0.01$, and ***$p < 0.001$.

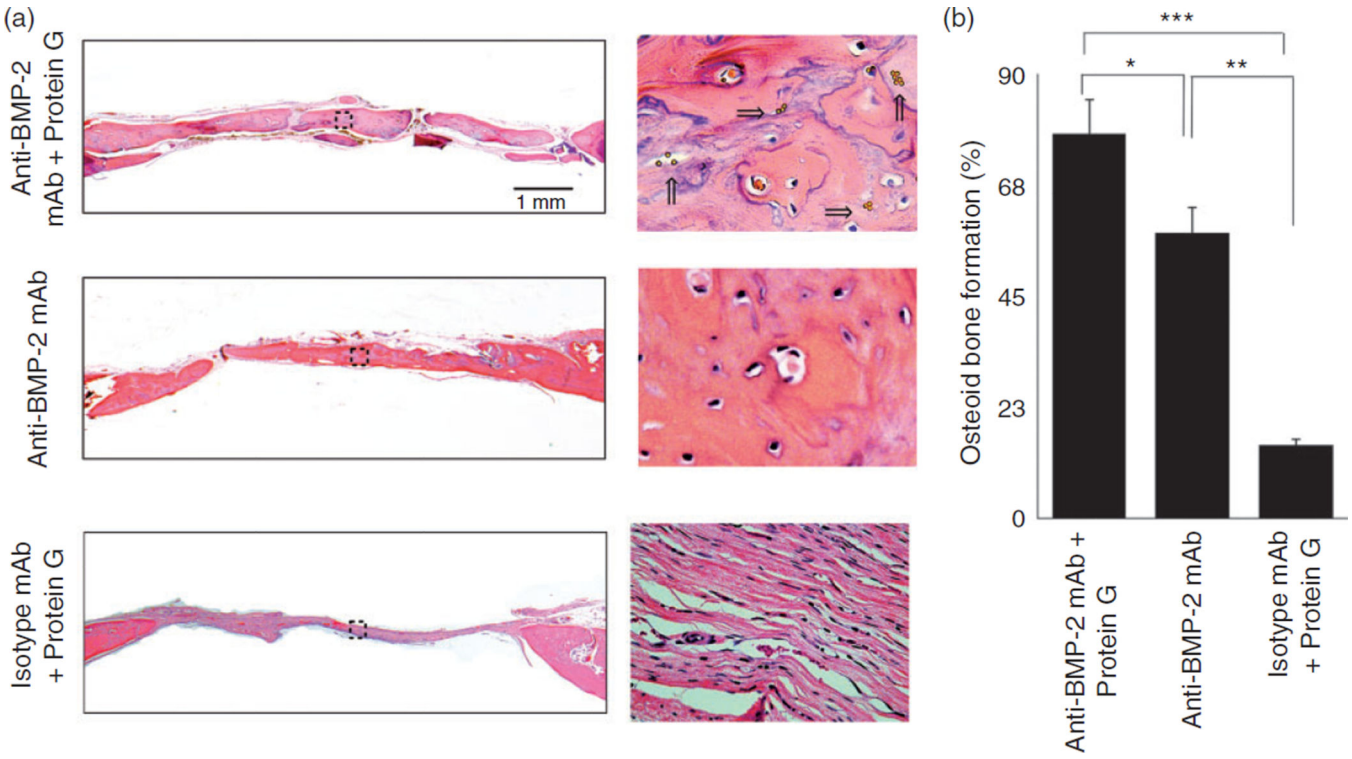

Figure 5.

Histological analysis of rat calvarial bone defects implanted withanti-BMP-2 mAb immobilized on ACS with or without Protein G-coupled microbeads linker. Protein G-coupled microbeads (yellow dots) are shown with arrows. Animals were sacrificed at 8 weeks after surgery and calvarial bones were processed for histologic and Histomorphometric analysis. (a) Histomicrographs in low (4×) and high magnification (40×) of H&E stained calvaria. (b) Histomorphometric analysis was performed on H&E stained sections and percentage of new bone formation was quantified. The percentage of osteoid bone coverage was measured within histomicrographs by histomorphometric analysis. *$p < 0.05$, **$p < 0.01$, and ***$p < 0.001$.

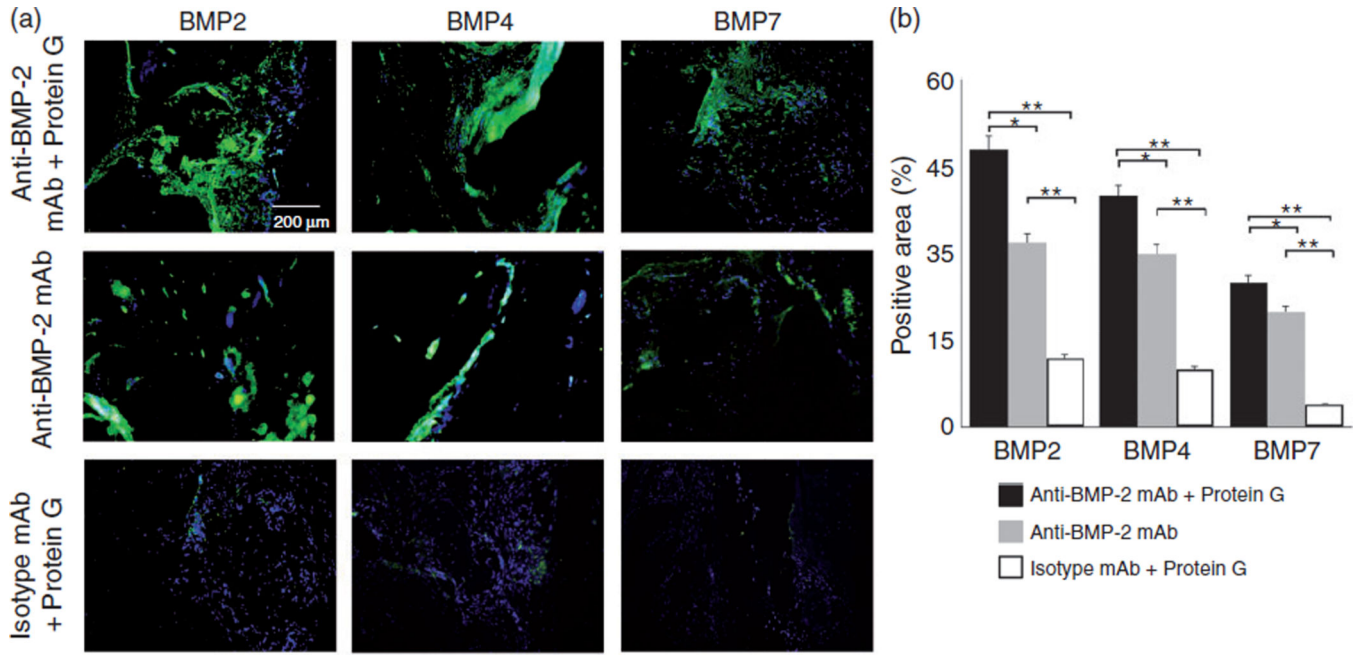

Figure 6.

Immunofluorescence labeling of tissue specimens harvested from rat calvarial bone defects implanted with anti-BMP-2 mAb immobilized on ACS with or without Protein G linker. Primary antibodies included those with specificity against BMP-2, -4, and -7. (a) Representative immunofluorescent CLSM images demonstrated positive labeling within sites implanted with anti-BMP-2 mAb immobilized on ACS with rec-Protein G linker, as well those sites with anti-BMP-2 mAb immobilized directly on ACS. (b) Analysis of the percentage of positively stained area for anti-BMP-2, -4, and -7 antibodies, showing that G protein-anti-BMP2 mAb complex presented the highest expression of BMP-2, -4, and -7 proteins in comparison to those sites with anti-BMP-2 mAb immobilized directly on ACS, or isotype-matched control mAb, $*p < 0.05$ and $**p < 0.01$, respectively.

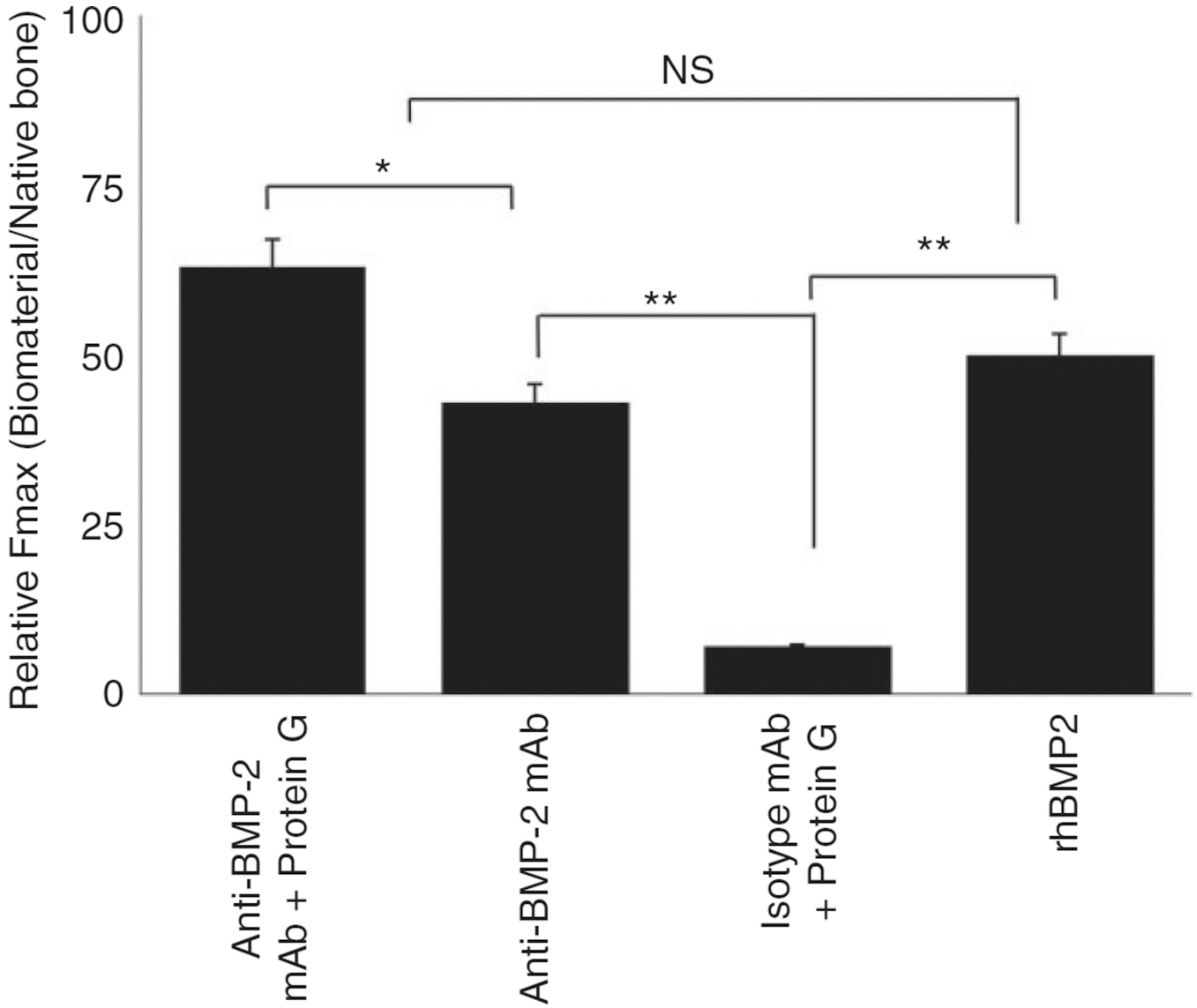

Figure 7.

Results of biomechanical evaluation of the regenerated bone and comparative analysis of strength of the newly formed bone in comparison to native bone.

*$p < 0.05$.

NS: not significant.